Toroidal rotation induced by 4.6 GHz lower hybrid current drive on EAST tokamak*

Xiang-Hui Yin(尹相辉)[1,2], Jun Chen(陈俊)[1,2], Rui-Ji Hu(胡睿佶)[1,2], Ying-Ying Li(李颖颖)[1], Fu-Di Wang(王福地)[1], Jia Fu(符佳)[1], Bo-Jiang Ding(丁伯江)[1], Mao Wang(王茂)[1], Fu-Kun Liu(刘甫坤)[1], Qing Zang(臧庆)[1], Yue-Jiang Shi(石跃江)[1,3], Bo Lyu(吕波)[1,†], Bao-Nian Wan(万宝年)[1], and EAST team

[1] *Institute of Plasma Physics, Chinese Academy of Sciences, Hefei* 230031, *China*
[2] *School of Nuclear Science and Technology, University of Science and Technology of China, Hefei* 230026, *China*
[3] *Department of Nuclear Engineering, Seoul National University, Seoul* 151-742, *Korea*

(Received 9 February 2017; revised manuscript received 10 July 2017; published online 30 September 2017)

Using a tangentially viewing x-ray imaging crystal spectrometer, substantial co-current rotation driven by lower hybrid current drive (LHCD) at 4.6 GHz is observed on EAST tokamak. This study presents plasma rotation behaviors with 4.6 GHz LHCD injection. Typically, the 10–20 km/s co-current rotation change and the transport of rotation velocity from edge to core are observed. The relationship between plasma parameters and rotation is also investigated, indicating that rotation decreases with increasing internal inductance (l_i) and increases with increasing safety factor (q_0). Hysteresis between rotation and T_e plasma stored energy is observed, suggesting different response times between the electron heating and rotation acceleration by LHCD. A comparison between the rotations driven by 4.6 G LHCD and 2.45 G LHCD on EAST is also presented, in which higher frequency LHCD could induce more rotation changes.

Keywords: intrinsic rotation, lower hybrid current drive (LHCD)

PACS: 52.30.−q, 52.35.Hr **DOI:** 10.1088/1674-1056/26/11/115203

1. Introduction

Rotation and its shear play important roles in tokamak plasmas since they can reduce the MHD instabilities[1,2] and enhance the confinement.[3,4] At present, rotation is driven mostly by direct neutral beam injection (NBI) momentum injection in most tokamak devices, which is predicted to not be efficient on ITER and future reactors because of the large machine size, high plasma density, and high beam energy.[5] Hence, the study of the rotation without external momentum injection, the so-called "intrinsic rotation", is important for improving predictions for plasma rotation in ITER and future fusion reactors. As one of the intrinsic rotation driving methods, LHCD-driven rotation has been reported on Alcator C-mod,[6–8] JT-60U,[9] Supra Tore,[10,11] and EAST[12] to induce significant toroidal rotation either in co- or counter-current.

The mechanism for LHCD rotation driving has been studied extensively and several key means were proposed. Change in residual stress through its dependence on magnetic shear was thought to be one of the driven mechanisms in both Supra Tore and Alcator C-mod.[6,10] A radial electric field created by the ripple-induced loss of thermal electrons could also drive rotation via the radial force balance equation.[10] Additionally, the radial electric field can also be generated by the outward motion of the electrons, which are driven by balancing the parallel momentum deposited in fast resonant electrons.[13–15] The LH wave injected momentum is one of the considered mechanisms, but this was calculated to be small.[6–10] Pfirsch-Schluter (PS) flows, which may be caused by the fast change of edge rotation, could induce drift flows in toroidal geometry.[12] As there remains much work to do on the LHCD rotation driving mechanisms, more experimental results in different devices should be analyzed for the more precise understanding of the LH-driven rotation.

On EAST, LHCD induced plasma rotation was studied for 2.45 GHz LHCD system previously.[12] A new 4.6 GHz LHCD system was deployed on EAST[16,17] in 2014, which provided new resources for plasma rotation studies at different LHCD frequencies.[18] Besides, with the improvement of the diagnostics on EAST, more information during LHCD injection became available. In this paper, the typical characteristics of the 4.6 GHz LHCD-driven rotation are presented. The preliminary analyses of LHCD induced rotation and its dependence on plasma parameters are performed.

The rest of this paper is organized as follows. In Section 2 the experimental setup on EAST is described. In Section 3 the rotation measurements during 4.6 GHz LHCD injection are presented. Finally, some conclusions are drawn from the present study in Section 4.

*Project supported by the National Magnetic Confinement Fusion Science Program of China (Grant Nos. 2013GB112004 and 2015GB103002), the National Natural Science Foundation of China (Grant Nos. 11405212 and 11261140328), and the Major Program of Development Foundation of Hefei Center for Physical Science and Technology China (Grant No. 2016FXZY008).

†Corresponding author. E-mail: blu@ipp.ac.cn

© 2017 Chinese Physical Society and IOP Publishing Ltd

2. Experiment setup

The experiments on plasma rotation were performed on EAST, which is equipped with fully superconducting magnets (major radius $R \sim 1.85$ m, minor radius $a \sim 0.45$ m, magnetic field $Bt_0 < 3.5$ T, plasma current $I_p < 1$ MA) with flexible magnetic configurations (diverted and limited) and advanced wall conditioning techniques for long-pulse high-performance operations.[16,17] In addition to the existing 2.45 GHz LHCD system, a new LHCD system operating at 4.6 GHz, capable of delivering up to 6 MW source power with the parallel index of refraction $n_{\|}$ in the range 1.8–2.23 was successfully commissioned in 2014.[19] Toroidal rotation was measured by the tangential high-resolution x-ray imaging crystal spectrometer (XCS), based on the Doppler shift of helium-like argon line (Ar XVII) in a wavelength range from 3.9494 Å to 3.9944 Å.[20,21] Typical time and spatial resolution for XCS are 10–100 ms and 1 cm, respectively. Electron temperature and density ($\rho = 0$–1.1) are obtained from Thomson scattering (TS) with spatial resolution up to ~ 1.0 cm and time resolution up to 20 ms.[22–24]

2.1. Experiment observation of 4.6 GHz LHCD induced plasma rotation

Development of the 4.6 GHz LHCD system on EAST adds the extra capability for non-inductive current drive, which also provides a tool for studying RF-driven rotation physics. Shown in Fig. 1 are time histories of plasma parameters for a 1.75 T ($R = 1.89$ m), 500 KA ($q_{95} = 3.7$) lower-single-null (LSN) L-mode discharge (shot #56028) with $P_{\rm LHCD} \sim 1.8$ MW ($n_{\|} = 2.26$) injected from 2.65 s to 8.3 s. The line-averaged electron density is held at $\sim 2.3 \times 1019$ m^{-3} with feedback control. Immediate drop in loop voltage ($V_{\rm loop}$) is seen upon the onset of LHCD, indicating that the current is efficiently driven by LHCD and the Ware pinch effect on the plasma rotation can be ignored. There is also 6.4% drop in the internal inductance (l_i) determined from EFIT reconstruction[25] and 12% increase in q_0, suggesting the effect of LHCD on the current density profile. Upon LHCD injection, the diamagnetic energy ($W_{\rm mhd}$) (~ 200 ms) and electron temperature (T_e) (~ 200 ms) increase substantially, while ion temperature (T_i) keeps nearly unchanged. For plasma core rotation, a co-current change of ~ 18 km/s is driven by LHCD on a time scale (~ 300 ms) slower than the variation time of the plasma temperatures. The difference shows that LHCD drives the rotation in an indirect mechanism. In other words, LHCD momentum injection[10,11] is not the main mechanism in LHCD driven rotation on EAST.

Figure 2 shows the profiles of the T_e, n_e, and δu_ϕ at different times ($t = 2.5$ s before 4.6 GHz, and $t = 2.7$ s/2.8 s/2.9 s, during LHCD) for the same discharge. It can be seen that T_e increases immediately with obvious gradient changing after the application of the 4.6 GHz LHCD, and the profiles of electron temperature become more peaked. As shown in Fig. 2(c), in the observed region of the XCS, δu_ϕ around $\rho \sim 0.3$ increases faster than in the core region, which indicates the existence of the transport of rotation from $\rho \sim 0.3$ to the core of the plasma and is consistent with the result in the 2.45 GHz LHCD discharge.[12]

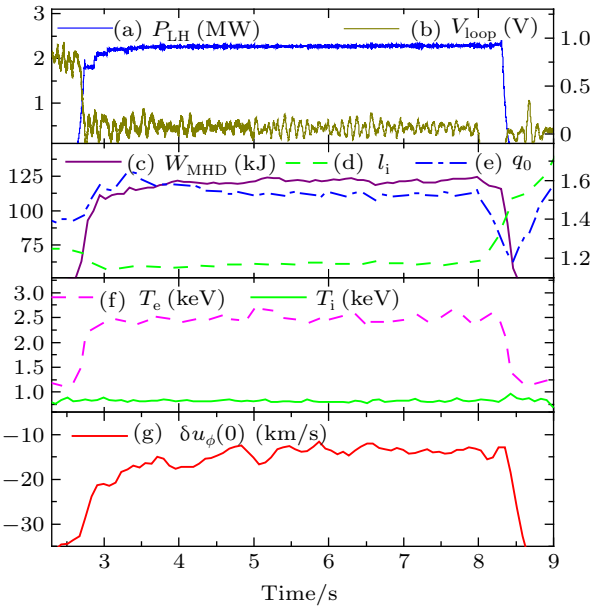


Fig. 1. (color online) Waveforms of an LSD 4.6 GHz LHCD shot (#56026) on EAST: (a) LHCD power, (b) loop voltage, (c) internal inductance, (d) diamagnetic energy, (e) central safety factor q_0, (f) central ion and electron temperature, and (g) central velocity.

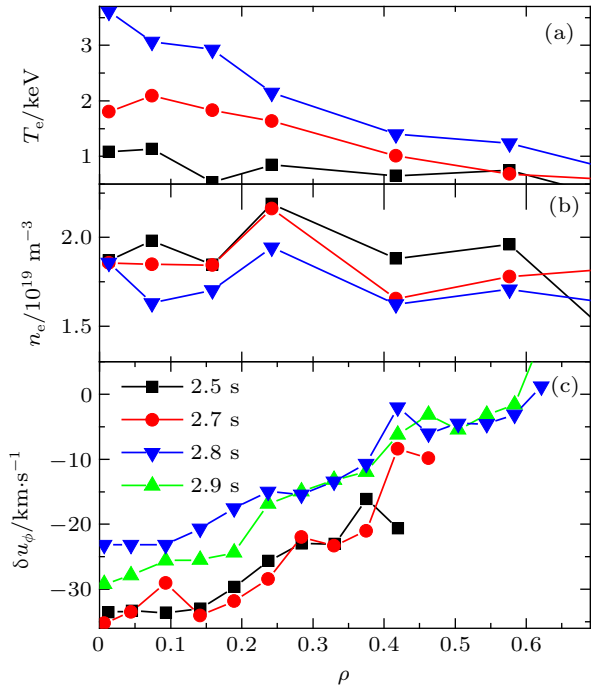


Fig. 2. (color online) Profiles of (a) T_e, (b) n_e, and (c) δu_ϕ for Shot #56026.

A comparison of LHCD rotation drive among different frequencies is carried out by injecting LHCDs of 2.45 GHz

and 4.6 GHz at different times during the L-mod discharge.[18] Figure 3 shows the experimental results for one discharge with 2.45 GHz and 4.6 GHz LHCD at a similar injected power, while electron density and plasma current are kept unchanged. It could be seen that the differences in loop voltage ($V_{\rm loop}$) and plasma stored energy are obvious between two subsequent injection periods, which indicates better current driven and heating efficiency for 4.6 GHz LHCD. Also, from the rotation measurements, larger rotation change is also observed for 4.6 GHz, i.e., there is ~ 3 km/s increment over 2.45 GHz results.

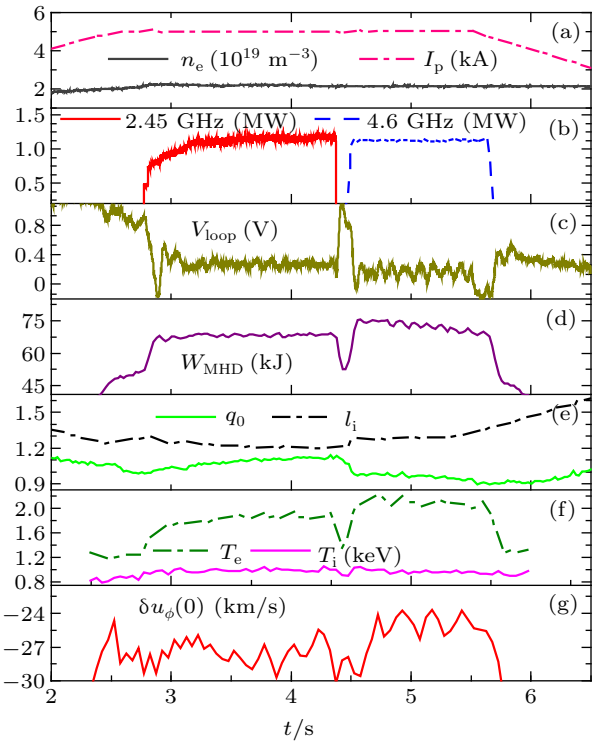


Fig. 3. (color online) Waveforms of an LSD LHCD shot (#54439) on EAST: (a) plasma current and line averaged electron density, (b) LHCD power, (c) loop voltage, (d) diamagnetic energy, (e) internal inductance and central safety factor q_0, (f) central ion and electron temperature, and (g) core relative to roidal rotation.

The profiles of the electron temperature, ion temperature and change of toroidal rotation in three conditions (ohmic condition, 2.45 GHz LHCD injection and 4.6 GHz LHCD injection) of this discharge are displayed in Fig. 4. It shows that 4.6 GHz LHCD has a stronger electron heating and rotation driving efficiency in the observed region ($\rho < 0.6$) than 2.45 GHz LHCD, while no big difference is observed between two LHCD discharges in ion heating. During the injection of the 2.45 GHz LHCD in the shot, the rotation driven by the LHCD is located in the edge region ($\rho > 0.4$), while the rotation in the whole profile changes with the injection of the 4.6 GHz LHCD. The difference may be related to the power deposition. The simulated deposition profiles[18] showed that 4.6 GHz LHCD was absorbed around $\rho = 0.3$ and $\rho = 0.6$, while the 2.45 GHz LHCD was absorbed in the $\rho = 0.6$ region.

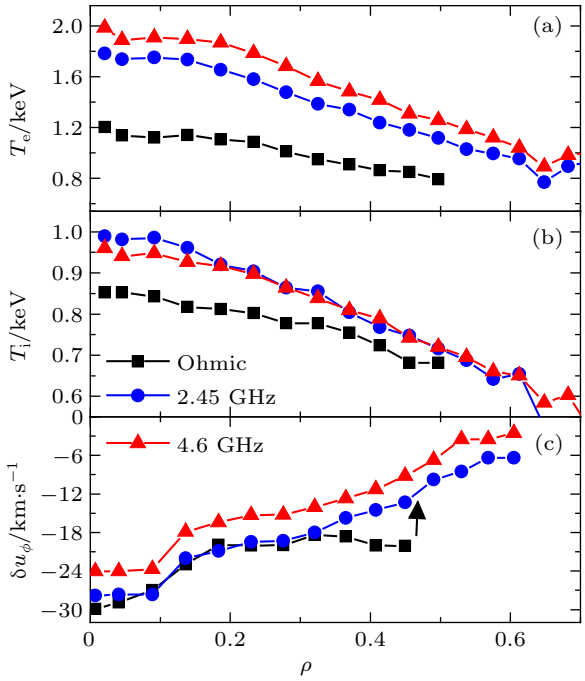


Fig. 4. (color online) Profiles of (a) electron temperature, (b) ion temperature, and (c) change in toroidal rotation under three different discharge conditions.

In Fig. 5, waveforms of three similar LSN LHCD discharges with different LHCD powers (1 MW, 1.5 MW, and 1.8 MW, respectively) are presented. It can be seen in Fig. 5(c) that the rotation increment increases with LHCD power increasing, just as seen on JT-60U[9] and C-mod.[6,8]

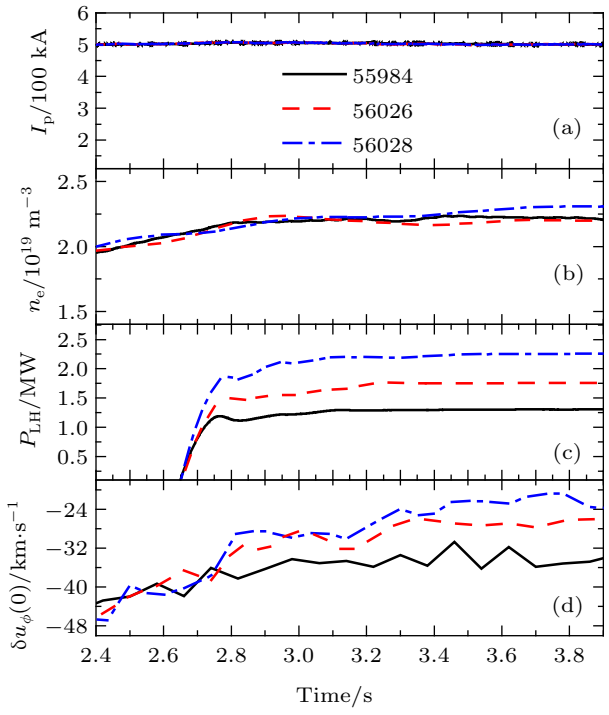


Fig. 5. (color online) Waveforms of three LSN 4.6 GHz LHCD shots (#55984, #56026, #56028) on EAST: (a) plasma current, (b) line averaged electron density, (c) power of 4.6 GHz LHCD, and (d) rotation velocity.

To further study the parametric dependence, the relationships between rotation increment and various parameters during the three shots are obtained and summarized in Fig. 6. An obvious hysteresis between the rotation velocity and T_e is shown in Fig. 6(a). Additionally, the amplitudes of change in electron temperature and rotation increase with the LHCD power increasing, while the slope between the two parameters is almost kept unchanged. The phenomena show the different time scales of electron heating and ion rotation velocity change induced by LHCD and the time scales of the two processes are independent of LHCD power. In Fig. 6(b), variations of rotation change with W_{mhd} show similar trends to that with T_e and a weak hysteresis between the rotation velocity and diamagnetic energy. The hysteresis shows that the rotation is driven mainly in an indirect way.

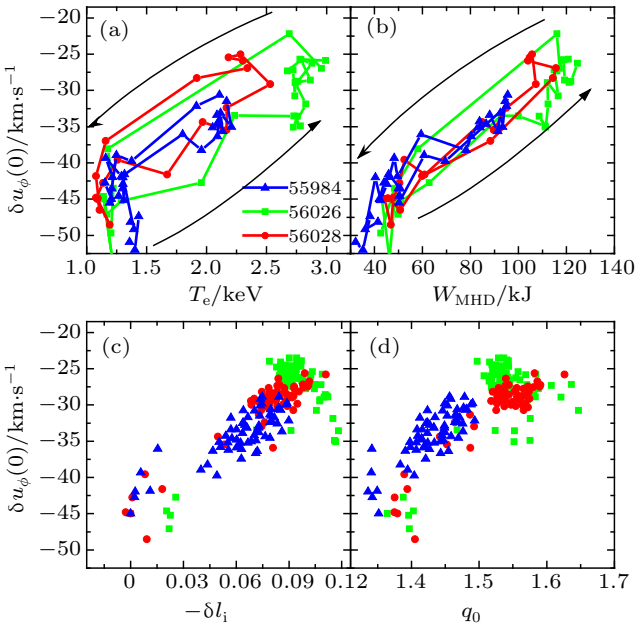


Fig. 6. (color online) Variations of trajectory in the core relative to roidal rotation δu_ϕ with (a) T_e/T_i and (b) W_{mhd} for discharges with LHW at varying power; core relative to roidal rotation versus (c) delta internal inductance δl_i, (d) q_0 for discharges with LHW at varying power.

With the improvement of the XCS system, the relationship between the increment of co-current toroidal rotation and the decrement in the internal inductance l_i, which is used to characterize the broadening of the current density profile induced by LHCD, is observed as shown in Fig. 6(c). The results were different from the previous results for the 2.45 GHz LHCD driven rotation on EAST,[12] which may be due to the limit to time resolution of the diagnostics at that time; and the results are similar to those observed on C-mod[8] except the different rotation direction. Figure 6(d) shows that the rotation increases with central safety factor q increasing. Both the increase of q and the decrease of l_i indicate that the flattening of the plasma current density profile plays an important role in accelerating toroidal rotation in LHCD discharge.

3. Conclusions

The experimental observations described above are similar to those of C-Mod,[6–8] JT-60U,[9] and Tore Supra.[10,11] Upon the upgrade of the diagnostic, the rotation evolution after LHCD injection can be observed. According to the observations of the time scale of the change on rotation, the direct mechanism for driving rotation for example, LH wave injected momentum, which contributes a small increment in counter-current direction,[10,11] is not the key factor in EAST. Like the results in the 2.45 GHz LHCD discharges,[12] the different time scales of change of the edge and core rotation show that the edge rotation may be the source of core rotation. The observed rotation change induced by LHCD is in the co-current direction and the amplitude is related to the power of the LHCD. One candidate mechanism is that the formation of the positive radial electric field induced by the injection of the LHCD[9–15] in the LHCD deposition region provides a co-current rotation drive force and then the change of the rotation transfers to the whole profile through momentum transport.

In summary, up to $\sim$ 20 km/s the co-current rotation increment is observed in the 4.6 GHz LHCD discharge. The rotation is transferred from the edge to the core region and increases with LHCD power increasing. The magnitude of the rotation is observed to increase with the electron temperature and stored energy increasing, and hysteresis between the parameters is observed. The hysteresis shows that the LHCD drive rotation is mainly in an indirect way. The rotation is well correlated with changes in the internal inductance, which is similar to the results of the C-mod experiment but in a different direction. Compared with the 2.45 GHz LHCD, 4.6 GHz LHCD can induce a slightly large rotation increment at the same power.

Acknowledgment

The authors wish to thank the diagnostic group, the vacuum group, the LHCD group and the operation team of EAST.

References

[1] Bondeson A and Ward D J 1994 *Phys. Rev. Lett.* **72** 2709
[2] Betti R and Freidberg J P 1995 *Phys. Rev. Lett.* **74** 2949
[3] Craddock G G and Diamond P H 1991 *Phys. Rev. Lett.* **67** 1535
[4] Terry P W 2000 *Rev. Mod. Phys.* **72** 109
[5] Doyle E J, Houlberg W A, Kamada Y, *et al.* 2007 *Nucl. Fusion* **47** S18-S127
[6] Rice J E, Podpaly Y A, Reinke M L, *et al.* 2013 *Nucl. Fusion* **53** 093015
[7] Rice J E, Ince-Cushman A C, Bonoli P T, *et al.* 2009 *Nucl. Fusion* **49** 025004
[8] Ince-Cushman A, Rice J, Reinkeet M, *et al.* 2009 *Phys. Rev. Lett.* **102** 035002
[9] Koide Y, Tuda T, Ushigusa K, *et al.* 1992 *Plasma Phys. Control. Nucl. Fusion Res.* **1** 777
[10] Chouli B, Fenzi C, Garbet X, *et al.* 2014 *Plasma Phys. Control. F* **56** 095018
[11] Chouli B, Fenzi C, Garbet X, *et al.* 2015 *Plasma Phys. Control. F* **57** 125007

[12] Shi Y, Xu G, Wang F, *et al.* 2011 *Phys. Rev. Lett.* **106** 235001
[13] Gao Z, Fisch N J and Qin H 2011 *Phys. Plasmas* **18** 082507
[14] Wang S 2011 *Phys. Plasmas* **18** 102502
[15] Zuo Y, Wang S and Pan C 2012 *Phys. Plasmas* **19** 102505
[16] Wan B N, Li J G, Guo H Y, *et al.* 2013 *Nucl. Fusion* **53** 104006
[17] Wan B N, Li J G, Guo H Y, *et al.* 2015 *Nucl. Fusion* **55** 104015
[18] Li M H, Ding B J, Liu F K, *et al.* 2016 *Phys. Plasmas* **23** 102512
[19] Wang F D, Shi Y J, Zhang W, *et al.* 2011 *J. Korean Phys. Soc.* **59** 2734
[20] Lu B, Shi Y J, Wang F D, *et al.* 2013 *Plasma Sci. Technol.* **15** 97
[21] Lyu B, Wang F D, Pan X Y, *et al.* 2014 *Rev. Sci. Instrum.* **85** 11E406
[22] Shao C Q, Zhao J Y, Zang Q, *et al.* 2014 *Plasma Sci. Technol.* **16** 721
[23] Zang Q, Zhao J Y, Yang L, *et al.* 2010 *Plasma Sci. Technol.* **12** 144
[24] Zang Q, Zhao J Y, Yang L, *et al.* 2011 *Rev. Sci. Instrum.* **82** 063502
[25] Zhang R R, Xiao B J and Luo Z P 2014 *Plasma Sci. Technol.* **16** 396